



Bacterial community structure and resilience are partially restored after 30 years of rehabilitation of an agricultural riparian system



Tolulope G. Mafa-Attoye ^a, Dasiel Obregon ^a, Micaela Tosi ^a, Maren Oelbermann ^b, Naresh V. Thevathasan ^a, Kari E. Dunfield ^{a,*}

^a School of Environmental Sciences, University of Guelph, Guelph, ON, Canada

^b School of Environment, Resources and Sustainability, University of Waterloo, Waterloo, ON, Canada

ARTICLE INFO

Keywords:
 Bacterial network
 Conservation
 Disturbance
 Network robustness
 Land management
 Restoration
 Soil microbiome

ABSTRACT

Soil microbiomes play critical roles in maintaining soil ecosystem functions, and therefore, they can be indicators of ecosystem recovery during the rehabilitation of degraded land. This study compared microbial community structure and co-occurrence patterns of potentially active bacterial communities in soils from a disturbance gradient: disturbed agricultural land (AGR), previously disturbed rehabilitated agroforest (RHF), and undisturbed natural forest (UNF). We quantified DNA and cDNA using qPCR and performed high-throughput amplicon sequencing to target potentially active bacterial communities. Bacterial transcript abundance was significantly higher in UNF compared to AGR, and the composition of potentially active bacterial communities varied significantly along the disturbance gradient. Soil temperature, nitrate, pH, carbon-to-nitrogen ratio, and total carbon were key soil properties driving differences in bacterial community composition. Key taxa such as *Burkholderiales*, *Haliangium*, and *Pseudomonas*, were differentially abundant along the disturbance gradient. Network robustness was used to evaluate network resilience and was highest in UNF, lowest in AGR, and RHF was intermediate, suggesting partial recovery of RHF following disturbance. Hub taxa from AGR were oligotrophs mainly from the phylum Actinomyceota, while forest soils hubs were from the phylum Pseudomonadota. UNF was the only site to have copiotrophic hub taxa such as *TRA3-20*, reflecting a functionally diverse network assembly in the nutrient-rich and less disturbed conditions. These findings show that after 30 years of rehabilitation the RHF has a similarity to UNF in terms of microbial abundance, composition, and soil characteristics, suggesting a recovery in ecosystem functionality at the site.

1. Introduction

In agricultural landscapes, intensive practices such as tillage, chemical fertilization, and excessive grazing disturb soil ecosystems (Price et al., 2021; Karimi et al., 2019). These practices contribute to biodiversity loss, soil degradation, and impaired ecosystem functions (Banerjee et al., 2019; Yu et al., 2022). At the boundary of these landscapes, riparian zones emerge as vital ecosystems, playing crucial roles in maintaining biodiversity and ecosystem structure (Lind et al., 2019; Graziano et al., 2022). However, disturbances from human activities and climate change can degrade riparian zones and disrupt the stability of microbial communities in these zones (Vitousek et al., 1997; Philippot et al., 2021). The rehabilitation of degraded riparian zones is crucial for restoring ecological functions to levels comparable to those of natural, undisturbed forests (Atkinson et al., 2022).

Restoring the stability and functioning of ecosystems is intricately linked to microbial composition and the complex ecological associations within microbial communities (Graziano et al., 2022; Philippot et al., 2021, Röttjers and Faust, 2018; Ma et al., 2020). These communities are instrumental in driving biogeochemical cycling, decomposition of organic matter, and plant-microbe interactions, which are key components in ecosystem restoration (Zhou et al., 2011). Studies that rely on taxonomic diversity as a bioindicator to assess the impact of disturbance on microbial communities have had significant limitations, such as the inability to detect early shifts and the varied responses to physical disturbances (Karimi et al., 2017).

Microbial communities are notable for their resilience, attributed to their small size and short generation times, allowing rapid adaptation to environmental changes (Allison and Martiny, 2008). This resilience is crucial for the adaptation and functional recovery of microbial

* Corresponding author.

E-mail address: dunfield@uoguelph.ca (K.E. Dunfield).

communities after disturbance (Hutchins et al., 2019). Therefore, a more comprehensive approach that evaluates changes in microbial communities through microbial networks has been proposed. This method provides a deeper insight into species co-occurrence patterns and the mechanisms of community assembly and stability (Karimi et al., 2017; Hernandez et al., 2021).

Network robustness, which measures a network's resilience to extinction cascades caused by species removal, assesses a network's capability to maintain connectivity and functionality in the face of disturbances or intentional attacks (Landi et al., 2018; Yu et al., 2022; Wang et al., 2023). These studies often use DNA-based methods; however, DNA alone cannot distinguish between live, dormant, or dead cells, potentially masking short-term responses to environmental change. RNA-based approaches targeting 16S rRNA transcripts offer a closer representation of the metabolically active fraction of the community (Blazewicz et al., 2013; Baldrian et al., 2012). Therefore, in this study, we reverse-transcribe and then sequence the complementary DNA (cDNA) from soil RNA extracts to characterize the potentially active communities. Since some dormant taxa may retain high ribosome content, and the relationship between rRNA levels and metabolic activity may vary among taxa and over time (Blazewicz et al., 2013), we therefore interpret cDNA-based profiles as "potentially active" populations rather than direct evidence of active metabolism.

In this context, we compared the microbial community structure and co-occurrence patterns of potentially active soil bacteria across a gradient consisting of "disturbed" agricultural land, "previously disturbed" rehabilitated agroforest, and undisturbed natural forest along Washington Creek (Fig. 1). The field site is a riparian zone degraded by agricultural intensification. Rehabilitation began in 1985, when trees were planted along a 1.6 km stretch of the creek to restore the riparian zone and reverse the damage caused by agricultural activities (Oelbermann and Gordon, 2008). Since then, several studies have evaluated biophysical changes and ecosystem services, such as water quality, greenhouse gas emissions, and carbon sequestration, demonstrating there has been a restoration of ecosystem services over time in the rehabilitated system (Oelbermann et al., 2008; De Carlo et al., 2019; Mafa-Attoye et al., 2020; Borden et al., 2021; Hundal et al., 2024). Moreover, Oelbermann and Gordon (2000), Oelbermann and Rimbault (2015) and Oelbermann et al. (2015) demonstrated increased organic matter input and elevated soil respiration at the RHF site relative to adjacent agricultural land. In our past work, we also established that shifts in plant diversity and functional root traits associated with

rehabilitation resulted in unique root-associated microbial communities (Mafa-Attoye et al., 2023). In the current study, we asked the following research questions: 1. Does potentially active bacterial community structure differ along this disturbance gradient? 2. Are there key taxa associated with each disturbance level? 3. How do bacterial networks and resilience vary across the disturbance gradient? We hypothesize that (1) lower nutrient levels in highly disturbed agricultural soils (AGR) will select for oligotrophic taxa, in contrast to the communities found in nutrient-rich forest soils and (2) microbial networks in less disturbed soils will exhibit greater connectivity and structural robustness compared to those in more disturbed environments.

2. Materials and methods

2.1. Site description

Washington Creek is an agriculturally dominated landscape in Oxford County, southern Ontario, Canada, and a tributary of the Grand River watershed. This 9-km long first-order spring-fed creek flows into the Nith River south of Plattsville (43°18'N 80°33'W). The area consists of riparian zones that serve as buffers for agricultural lands, connected by the same creek and situated on both sides of the creek. The climate is temperate, with a 30-year mean annual temperature of 7.3°C and mean annual precipitation of 919 mm (Environment and Climate Change Canada, 2020). Soils in Oxford County are classified as Grey Brown Luvisols with a silt loam or clay loam texture (Mozuraitis and Hagarty, 1996). Three sites were sampled across the landscape to represent a gradient of disturbance (disturbed, previously disturbed, and undisturbed sites). These sites include an agricultural land (AGR, disturbed), a rehabilitated agroforest (RHF, previously disturbed) adjacent to the AGR, and an undisturbed natural forest (UNF, undisturbed). The conventional agricultural land (AGR) is on a corn (*Zea mays* L.) and soybean (*Glycine max* L.) rotation and was planted with soybeans during the study. The RHF was formerly a degraded riparian zone due to agricultural intensification. Rehabilitation efforts and planting of trees along the 1.6-km section of the creek commenced in 1985. Perennial vegetations such as alder [*Alnus incana* subsp. *rugosa* (Du Roi) R.T. Clausen., *Alnus glutinosa* (L.) Gaertn., and *Alnus rubra* Bong.] and hybrid poplar (*Populus x canadensis* Moench) were planted at the inception of the rehabilitation process. Silver maple (*Acer saccharinum* L.) was planted as filler trees in the subsequent year and multiflora rosevine (*Rosa multiflora* Thunb.) and redosier dogwood (*Cornus sericea* subsp. *sericea* L.)

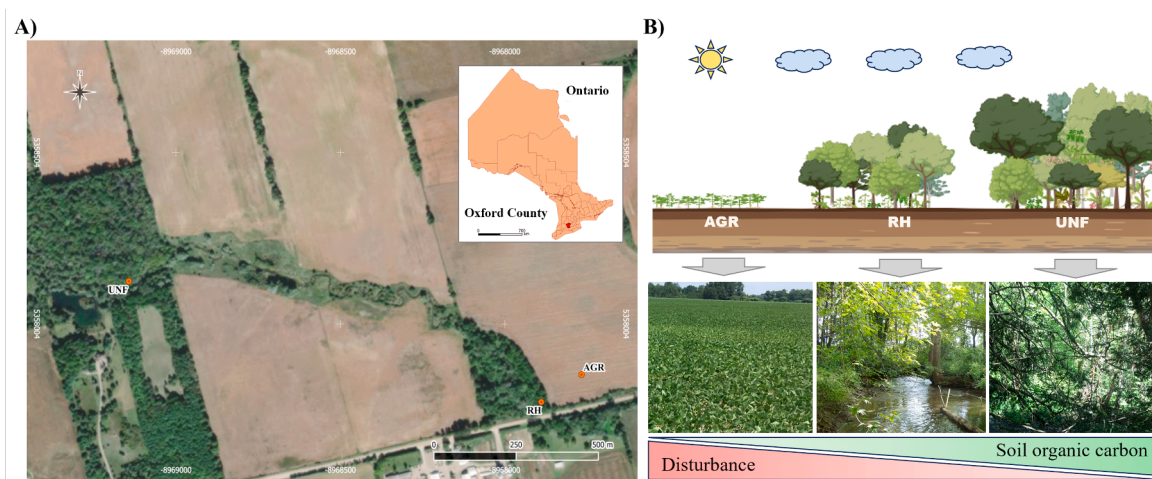


Fig. 1. Study site location and disturbance gradients. (A) An aerial map showing the geographical locations of different land use types in Washington Creek (approx. 43°18'N, 80°33'W); agricultural land (AGR), Rehabilitated Forest (RHF), and undisturbed natural forest (UNF). The map includes a small inset showing the location of Oxford County within Ontario. (B) Conceptual illustrations and site pictures of AGR "disturbed", RHF, "previously disturbed", and UNF, an Undisturbed Natural Forest. The diagram highlights the gradient of disturbance and soil carbon levels across these land uses.

were also planted between 1990 and 1991. More details of the site, rehabilitation efforts, and studies on soil microbial communities are found in Oelbermann and Gordon (2000), Oelbermann et al. (2008), and Mafa-Attaye et al. (2020), respectively. Likewise, the UNF, located approximately 320 m upstream of the RHF site, predominantly consists of vegetation such as American beech (*Fagus grandifolia* E.), sugar maple (*Acer saccharum* L.), basswood (*Tilia americana* L.), and eastern hemlock (*Tsuga canadensis*). This site has been undisturbed for over 150 years. At each site, the study area was 5 m from the edge of the creek and 30 m long and parallel and on one side of the creek for a total area of 150 m. Within each site, we established four spatially distinct replicate plots (1 m × 1 m) per site. Since no comparable streams with matching riparian zone age, vegetation structure, rehabilitation history and land-use practices were available within the study area, site-level replication was not possible. This limitation should be considered when extrapolating our results to other riparian or land-use contexts.

2.2. Soil sampling and physicochemical analyses

Soil samples were collected during the summer of 2018, on July 04 and August 15 from a depth of 0–10 cm using a sterile soil auger. The collection followed a Z-transect pattern within each plot to ensure representative sampling. The samples from each plot were combined into a sterile, labeled bag, and 2 g of the homogenized soil was immediately transferred into pre-weighed sterile tubes containing 3 mL of LifeGuard™ Soil Preservation Solution (Qiagen, Toronto, CA) to preserve RNA. Samples were then transported on ice to the lab and stored at –80°C before RNA extractions. A total of four replicates per site were collected on each sampling date (n = 8).

Ten grams of fresh soil samples were used to determine gravimetric moisture content (MC) through oven dry method. To measure soil pH, 10 g of soil was mixed with 10 mL of deionized water (1:1 soil-to-water ratio), stirred thoroughly, and allowed to sit for 1 h before pH was measured using a calibrated pH meter. The remaining subsampled soil was kept at –20°C. Total nitrogen (total N) and total carbon (total C) were analyzed with an elemental analyzer (CN 628, LECO Instruments, Canada). To analyze NO₃[–] and NH₄⁺, 5 g of soil was mixed with 25 mL of 2.0 M KCl. Using a reciprocating shaker, the solution was stirred for 30 min at 180 rpm, then filtered through the Whatman No. 42 filter paper. The extract was passed through a Shimadzu 1800 UV-Vis Spectrophotometer (Shimadzu Corp., Kyoto, Japan). Nitrate concentrations were measured at 540 nm after 12 h of color development using the Griess-Ilosvay method, while ammonium concentrations were determined at 650 nm after 1 h of color development using the indophenol blue method (Miranda et al., 2001).

2.3. Nucleic acid extraction

Soil samples preserved with LifeGuard™ were centrifuged at 2500 xg for 5 min to remove the preservative solution prior to extraction. Total soil RNA and DNA were co-extracted from soil samples using RNeasy PowerSoil Total RNA Isolation with DNA Elution Accessory Kits (Qiagen®, Valencia, CA) following the manufacturer's instructions. Reverse transcription into single-stranded complementary DNA (cDNA) was achieved using Applied Biosystems® High-Capacity cDNA Reverse Transcription Kit (Life Technologies Corp.) as described by the manufacturer. The DNA yield was quantified using Qubit® Fluorometric Quantitation (Invitrogen), and PCR inhibition assays were conducted to identify optimal ranges of template dilution for qPCR assays (Reardon et al., 2013). The resulting cDNA samples were stored at –20°C for further analysis.

2.4. Quantitative PCR

Total bacterial abundance (16S rRNA) was quantified using qPCR assays targeting the marker gene 16S rRNA in both DNA and cDNA. The

qPCR protocols were run in 20 μL reactions that contained 10 μL of 2X SsoFast™ EvaGreen® Supermix (Bio-Rad Laboratories, Inc.), 1 μL (10 μM) of each forward (338 F) and reverse (518 R) primers (Fierer et al., 2005), 2 μL of diluted template DNA and cDNA (1–10 ng/μL), and DNase-free water to make the final volume. A standard curve based on 1:10 dilutions of a plasmid DNA containing the target gene (16S rRNA) was used. All qPCR reactions were carried out in duplicate with reaction efficiencies of between 97 % and 102 % using the CFX96 Touch™ Real-Time PCR Detection System (Bio-Rad Laboratories, Inc.). The results were expressed as log gene and transcript copy numbers per g of dry soil (gene and transcript copy g^{–1}).

2.5. Amplicon sequencing

Samples of cDNA (~20 ng/μL) were sent to the Genome Quebec Innovation Centre at McGill University for high-throughput sequencing via the Illumina MiSeq platform (Illumina Inc., USA).

PCR amplification of the 16S rRNA V4 region was performed using primer pairs 515 F (Parada et al., 2016) and 806 R (Apprill et al., 2015) modified primers from the Earth Microbiome project (Thompson et al., 2017). Reactions were carried out in 25 μL volumes using KAPA HiFi HotStart ReadyMix, following standard thermocycling conditions provided by Genome Québec.

2.6. Bioinformatics pipeline

The demultiplexed sequences obtained from 250 bp paired-end reads on the Illumina MiSeq platform were processed using Quantitative Insights Into Microbial Ecology QIIME2 (version 2023.5) and its plugins (Bolyen et al., 2019). The DADA2 pipeline was used to clean and merge paired-end reads via q2-dada2 (Callahan et al., 2016), allowing sequence analysis resolution to the single-nucleotide level of amplicon sequence variants (ASVs). The alpha diversity metrics (i.e. Observed ASVs, and Pielou's Evenness) were computed using q2-diversity after samples were subsampled without replacement, and rarefaction curves were generated to assess adequacy of read depth. Taxonomic classification was conducted using the q2-feature-classifier classify-sklearn (Bokulich et al., 2018) with a classifier trained on the SILVA database v.138.(Quast et al., 2012) for bacterial reference sequences. The raw sequence data have been deposited in NCBI SRA under the project PRJNA718381.

2.7. Statistical analyses

To assess potential temporal effects, we compared soil physicochemical properties between the two sampling dates (July 4 and August 15, 2018) using two-way ANOVA. Since no significant differences were observed between dates (P > 0.05), data from both sampling events were pooled for subsequent analyses.

The differences between soil physicochemical properties including pH, MC, and total C were determined using one-way ANOVA. Likewise, qPCR data, including gene and transcript abundance (expressed as gene and transcript copy number g^{–1} dry soil), were compared across the disturbance gradient using a one-way ANOVA followed by Tukey's multiple comparison test ($\alpha = 0.05$), as these data met the assumptions of normality and homogeneity of variances. However, differences in alpha diversity metrics; Observed ASVs and Pielou's Evenness, were assessed using the non-parametric Kruskal-Wallis test ($\alpha = 0.05$), due to variations from normality commonly observed.

Differences in bacterial community structure among land uses were visualized using Principal Coordinates Analysis (PCoA) based on a Bray-Curtis dissimilarity matrix, and statistically evaluated using pairwise permutational multivariate analysis of variance (PERMANOVA) with the adonis function in the vegan package in R. Separate PERMANOVA tests were performed for each site pair (AGR-RHF, AGR-UNF, RHF-UNF). Beta dispersion, which evaluates the homogeneity of

multivariate dispersions, was estimated using the *betadisper* function, also from the Vegan package, in R (version 4.1.3). The numbers of shared amplicon sequence variants (ASVs) among the sites were visualized using Venn 2.1.0 executed in the online tool (Oliveros, 2015).

The relationship between soil properties and bacterial (gene and transcript) abundance was assessed using a Random Forest regression package in R (Liaw and Wiener, 2002). Feature importance was evaluated using the percentage increase in Mean Squared Error (%Inc MSE) to determine the most influential variables in predicting bacterial abundance based on DNA and cDNA data. Variables with negative %Inc MSE values, were excluded as they reduced model accuracy by introducing noise. Specifically, nitrate (NO_3^-) was excluded from DNA-based analysis, whereas NO_3^- , ammonium (NH_4^+), and pH were excluded from RNA-based (cDNA) analysis. To further assess the effect of soil properties on bacterial community composition, distance-based redundancy analysis (db-RDA, Legendre and Anderson, 1999), which accommodates non-Euclidean distance measures, was performed in R using the “Vegan” package, based on a Bray–Curtis dissimilarity matrix. The ordination was visualized using R package ggplot2. Soil properties were selected based on their ecological relevance and tested for collinearity. Variables such as bulk density, ammonium, total N, and moisture content with high Variance inflation factor ($\text{VIF} > 5$) values were omitted from the db-RDA plot due to collinearity.

Differences in taxa abundance among the sites were analyzed using the ANOVA-like differential expression package (ALDEx2) (Gloor et al., 2016) in R (ver. 4.1.3). This approach utilizes a centered log ratio (clr) transformation based on the geometric mean of read counts in the sample to determine the relative abundance (Aitchison, 1986). The comparisons were determined using the Kruskal–Wallis test, ($p < 0.01$) and heatmaps were produced using VEGAN (v. 3.1.0). Random Forest classification in MicrobiomeAnalyst was used to identify key bacterial taxa. This method ranked the most important bacterial taxa based on their contribution to the classification accuracy. Feature importance was evaluated using Mean Decrease Accuracy to highlight key indicator taxa that differentiate between sites (Chong et al., 2020).

2.7.1. 16S rRNA operon copy number

To infer ecological strategies of taxa, we used PICRUSt2 v2.4.1 to detect 16S rRNA operon copy numbers (Douglas et al., 2020). Denoised ASVs sequences were phylogenetically placed into a backbone tree of reference genomes with known rrn operon counts, and a phylogenetic generalized least squares model was applied to identify copy numbers for each ASV. Rrn copy numbers were merged with the ASV abundance table and collapsed counts at the genus level based on SILVA v138 taxonomy (Quast et al., 2012). For each soil sample, the community-weighted mean rrn copy number was computed by multiplying the rrn copy number of each ASV by its relative abundance, then summing the resulting values across all ASVs present in the sample, following the approach of Nemergut et al. (2016). Genera were classified as oligotrophs (predicted rrn operon copy number ≤ 2), copiotrophs (≥ 5), or intermediates (3–4) (Klappenbach et al., 2000), and number of taxa in each category were also summed for each sample.

2.7.2. Co-occurrence network analysis

Bacterial co-occurrence networks were constructed to explore potential relationships among taxa within each land use using the Sparse Correlations for Compositional data (SparCC) method (Friedman and Alm, 2012), implemented in R v. 3.6.3 (R Core Team, 2020). These networks represent statistical co-occurrence patterns based on positive correlations ($\text{SparCC} > 0.75$, $P\text{-value} < 0.05$). Topological features such as network diameter, average degree, weighted degree, modularity, number of modules, and average clustering coefficient were calculated to determine differences in the strength of the networks, and networks were visualized using the software Gephi 0.9.2. (Bastian et al., 2009) Eigenvector centrality (nodes with an eigencentrality value > 0.75) was employed to identify highly connected and influential nodes (hubs)

within the co-occurrence network. (Peschel et al., 2021). Reads from cDNA were filtered to retain ASVs with a minimum of 10 total reads across all samples before constructing the co-occurrence network. Using Venn diagrams, we identified pairs of taxa with conserved co-occurrence association across two or three land uses.

2.7.3. Network robustness

We modeled the robustness of the co-occurrence networks in response to “node removal” to determine how the removal of nodes impacts the overall network connectivity and resilience (Wang et al., 2023, Kratou et al., 2024). The node removal or “network attack tolerance” test, was performed using the NetSwan package (ver. 0.1). All nodes were subjected to four removal attack strategies: (i) Random removal, (ii) betweenness centrality (BNC), (iii) Degree and (iv) Cascading, (combination of Random and BNC) (Lee et al., 2022; Abuin-Denis et al., 2024). In random removal, nodes are removed without targeting specific characteristics, providing a baseline measure of network robustness. BNC removes nodes with high betweenness centrality, which are crucial for maintaining connectivity across the network. Degree centrality targets and removes high-degree nodes, which act as influential hubs for local network structure. Lastly, cascading simulates chain reactions, revealing the network’s vulnerability to compounding failures (Kim et al., 2019). Each strategy thus offers a distinct perspective on network resilience, collectively helping to evaluate microbial community robustness under diverse disturbances. While informative, these models are based on hypothetical node removal and should be interpreted as exploratory tools for understanding how network structure might respond to disturbance (Faust and Raes, 2012; Weiss et al., 2016).

For comparative purposes, we defined a threshold of 50 % connectivity loss as a benchmark of biological relevance. We assumed that within microbial ecosystems, this magnitude of loss of connectivity could signify a crucial tipping point, beyond which the microbial community may undergo drastic functional shifts or face systemic vulnerabilities (Ho et al., 2016; 2018). By adopting this 50 % threshold, we provide a clear metric of resilience to determine how many nodes need to be removed to achieve this 50 % loss in connectivity. Networks that require the removal of fewer nodes to reach this threshold are considered less robust (Landi et al., 2018). The igraph R package was utilized to create visual descriptions of the data (Csardi and Nepusz, 2006).

3. Results

3.1. Soil physicochemical properties associated with disturbance

The three land use types, agriculture (AGR), rehabilitated forest (RHF), and undisturbed natural forest (UNF), showed distinct physico-chemical properties that varied along the disturbance gradient ($P < 0.05$, Table 1, Fig S1). Significantly higher soil temperature and bulk density were recorded at the AGR site compared to the RHF and UNF sites (ANOVA, $P < 0.05$). In contrast, the UNF site had significantly higher moisture, total C, total N, and Ammonium (NH_4^+) compared to AGR and RHF ($P < 0.05$). In general, the soil properties at RHF were intermediate between those at UNF and AGR, except for soil pH, which was significantly higher at RHF (Table 1).

3.2. Bacterial abundance and diversity and rrn copy number

Bacterial gene abundance (DNA) as quantified by 16S rRNA gene copies per gram of dry soil was significantly higher in UNF and RHF sites compared to the AGR site ($P < 0.05$). Likewise, bacterial transcript abundance (cDNA) as quantified by 16S rRNA transcript copies per gram of dry soil was significantly higher in UNF compared to AGR ($P < 0.05$) (Fig. 2A). There were no significant differences in alpha diversity (Observed ASVs and Pielou's Evenness) between the land uses (Fig. 2B). However, the potentially active bacterial community composition as

Table 1

Soil physicochemical properties (0–10 cm depth) across disturbed agricultural land (AGR), previously disturbed rehabilitated agroforest (RHF), and undisturbed natural forest (UNF) at Washington Creek. Values are presented as the mean \pm SE. Values followed by the same letter within a row are not significantly different ($P \leq 0.05$, $n = 8$).

	Land uses		
	AGR	RHF	UNF
<u>Soil properties</u>			
Temperature°C	22.88 ± 1.20a	19.90 ± 0.26b	18.73 ± 0.21b
Grav. Moisture Content (%)	15 ± 0.01c	47 ± 0.05b	121 ± 0.20a
NH ₄ ⁺ (mg-N kg ⁻¹)	2.55 ± 0.59c	17.45	81.39 ± 18.02a ± 3.67b
NO ₃ (mg-N kg ⁻¹)	13.41 ± 1.05	24.84 ± 6.85	15.84 ± 4.83
Total N (g kg ⁻¹)	2.91 ± 0.06c	4.94 ± 0.50b	9.61 ± 0.80a
Total C (g kg ⁻¹)	29.07 ± 0.68c	71.85 ± 5.06b	143.47 ± 14.57a
Soil C: N Ratio	9.98b	14.54a	14.93a
pH	7.22 ± 0.05b	7.63 ± 0.02a	7.15 ± 0.07b
Bulk Density (g cm ⁻³)	1.13 ± 0.03a	0.93 ± 0.06b	0.544 ± 0.05c

determined by the Bray-Curtis dissimilarity matrix, showed significant variations across the disturbance gradient and land uses based on the PERMANOVA test ($F=1.55$, $P = 0.0001$). These differences are seen in Principal Coordinates Analysis (PCoA) plots (Fig. 2C). The pairwise PERMANOVA also indicated differences among the sites ($P < 0.05$) with no differences in multivariate dispersion across sites, as assessed using the betadisper function (Supplementary Table S1).

There were 382 shared ASVs observed across the land uses, with AGR

being the most distinct, having 122 unique ASVs, whereas RHF had 28 unique ASVs and UNF had 39. The two forested sites, UNF and RHF, shared the highest number of ASVs, totaling 135, however, RHF and AGR shared 75 ASVs and UNF and AGR shared 71 ASVs (Fig. 2D).

The majority of ASVs across all the land uses were classified as oligotrophs. AGR had the fewest copiotrophic taxa (9), RHF had 15 copiotrophic taxa and UNF had 13 (Table S2). The UNF site also had the fewest taxa that were identified as oligotrophs. The community weighted mean rrn copy number indicated that oligotrophs dominate in these systems, ranging from 1.20 in UNF, 1.22 in AGR and 1.27 in RHF (Figure S2).

3.3. Environmental factors driving microbial community abundance and structure

Random forest regression analysis revealed that several environmental variables including C: N, NH₄⁺, moisture content, bulk density, Total C, Total N, land use, temperature, and pH contributed to the prediction of total bacterial gene abundance (DNA). Among these, C: N, moisture, and land use were statistically significant with C: N having the highest %Inc MSE (percent increase in mean squared error) values (Fig. 3A, top panel). The same environmental variables except for NH₄⁺ and pH also contributed to the prediction of the abundance of the potentially active bacterial communities. For cDNA, none of the predictor variables were statistically significant ($P \leq 0.05$), although moisture content had the highest %IncMSE value (10) (Fig. 3A, bottom panel).

The distance-based redundancy analysis (db-RDA) revealed that

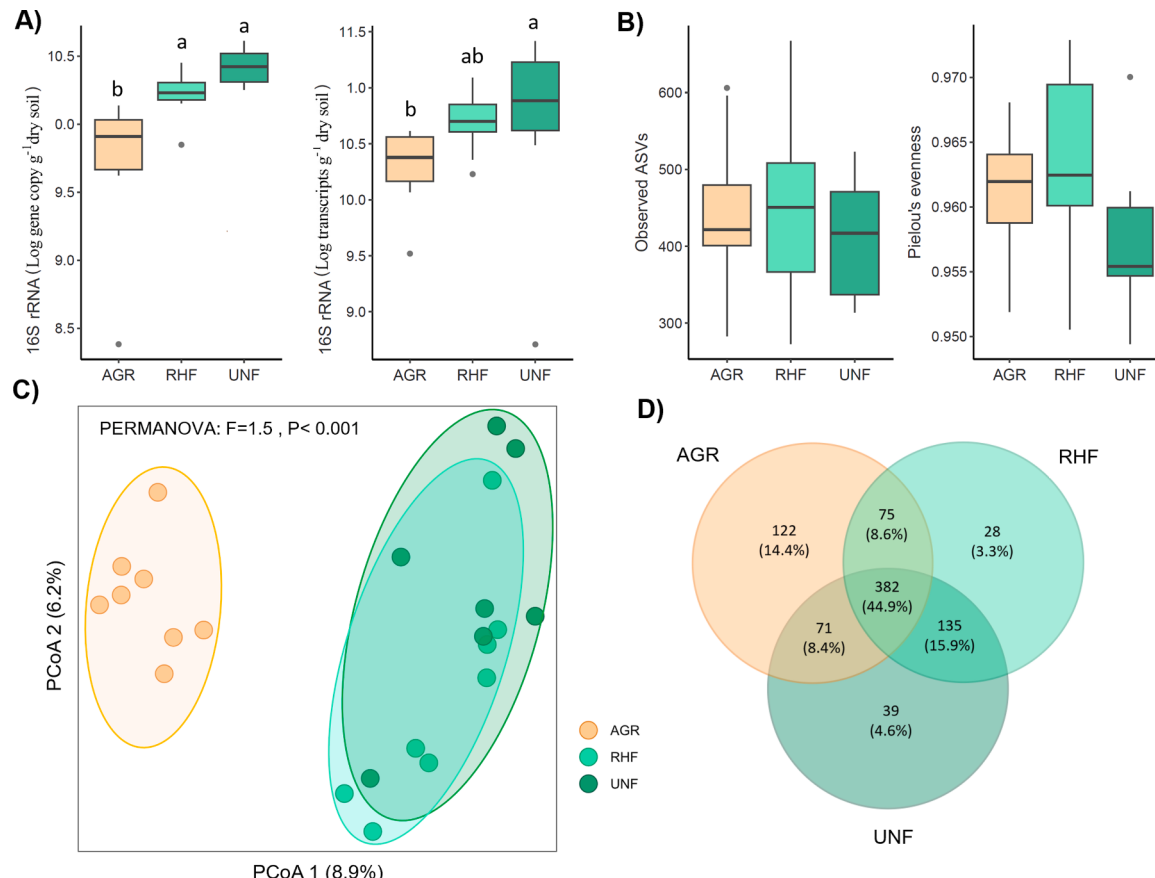


Fig. 2. Bacterial community structure across land use types: (A) Abundance of the total bacterial gene (16SrRNA) (DNA, on the left) and transcript (cDNA, on right). Different letters within the same group indicate significant differences between land uses (Tukey HSD, $P < 0.05$). (B) Bacterial alpha diversity as determined by Observed ASVs and Pielou's evenness across land use (C) Principal coordinate analysis (PCoA) plot based on Bray-Curtis distances showing the compositional differences between AGR, RHF, and UNF (D) Venn Diagram showing the number of shared and unique ASVs among land uses.

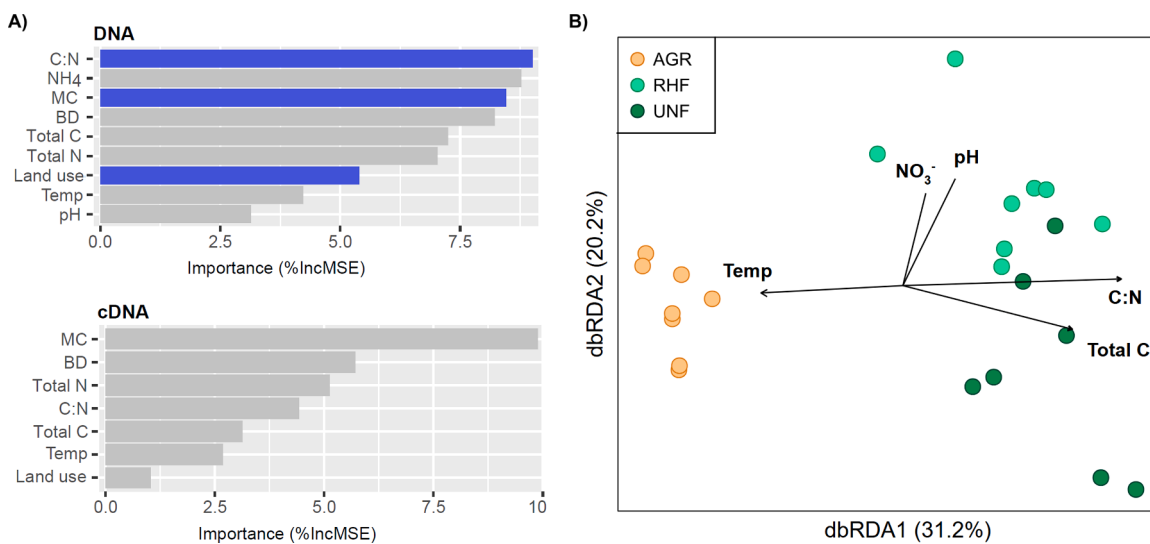


Fig. 3. Relationship between soil properties, bacterial abundance, and community composition: (A) Random Forest regression analysis showing the relative importance of abiotic factors in driving bacterial gene (DNA) and transcript (cDNA) abundances. The percentage increase in mean squared error (%IncMSE) indicates the contribution of each independent variable to prediction accuracy; higher %IncMSE values represent greater importance. Variables with negative %IncMSE values (NO_3^- in DNA analysis; NO_3^- , NH_4^+ , and pH in cDNA analysis) were excluded, as they reduced model accuracy. Significant predictors ($P \leq 0.05$) are indicated in blue. MC: Moisture content; BD: Bulk density. (B) Distance-based redundancy analysis (dbRDA) plot showing relationships between bacterial community composition and soil properties in AGR (brown), RHF (light green), and UNF (dark green). Soil factors are represented as vectors (black arrows). The length and direction of these vectors indicate the strength and direction of the relationship with the bacterial community. Total C: Total carbon, Temp: Temperature, NO_3^- : Nitrate, C: N; Carbon to Nitrogen ratio. N.B: Selection of soil properties was based on collinearity and ecological relevance therefore bulk density, ammonium, total nitrogen, and moisture content are omitted in the plot based on the Variance inflation factor (VIF).

about 50 % of the variation in bacterial community composition was explained by soil properties (Fig. 3B). The positioning of samples and vectors in the ordination space indicates that AGR samples were associated with higher temperature values, while RHF and UNF samples were associated with higher values of C:N ratio, total C, pH, and NO_3^- .

3.4. Shift in taxonomic composition

The dominant bacterial phyla across all sites were Pseudomonadota (Proteobacteria), Acidobacteriota, Planctomycetota, and Myxococcota (Fig. 4A). The distribution of the potentially active phyla differed among

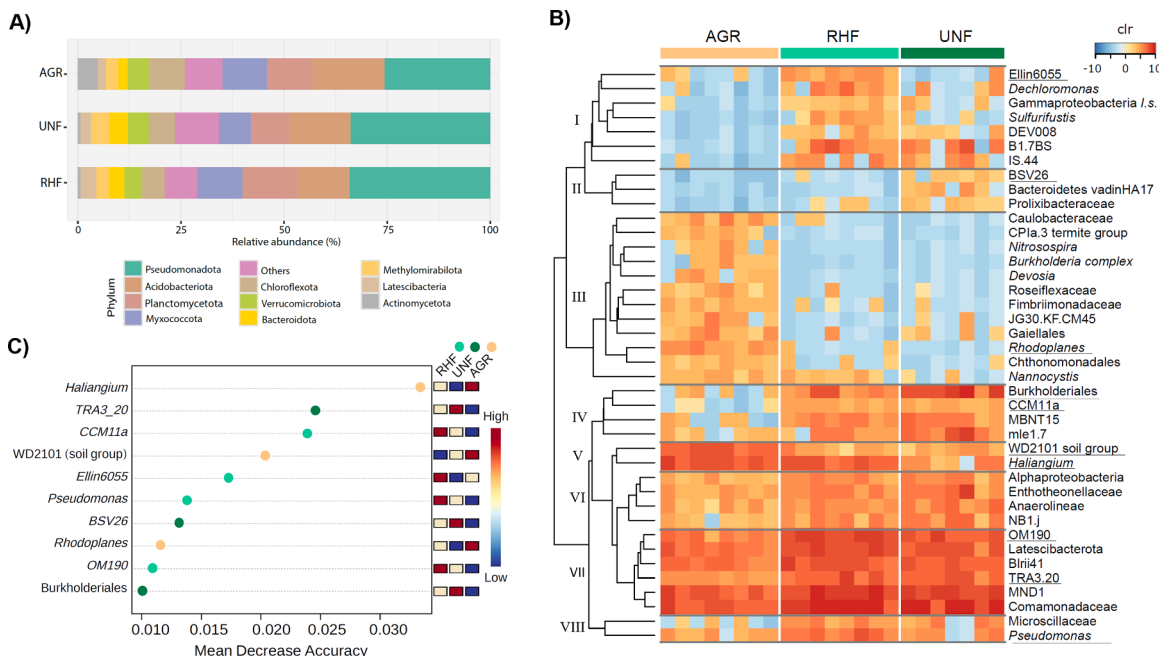


Fig. 4. Comparative analysis of bacterial taxonomic composition across land uses: (A) Relative abundance of the top 10 bacterial phyla across AGR, RHF, and UNF (B) Heatmap shows 40 differentially abundant bacterial genera (center log ratio (clr) transformed) and separated into clusters I-VII with grey delineations as determined by the ALDEX2 algorithm (Kruskal-Wallis test, $P < 0.01$) (C) Key indicator taxa that differentiate between land-use types determined using random forest classification. Taxa are ranked by Mean Decrease Accuracy, where higher values indicate greater importance for classification. The color gradient indicates relative abundance across sites (red = high, blue = low), and colored dots show the site where each taxon is most abundant. Taxa identified as indicator taxa in panel B are underlined in panel B.

land uses, AGR had a lower abundance of Pseudomonadota and a higher abundance of Actinomycetota compared to the RHF and UNF (Fig. 4A). In contrast, we observed lower abundances of Myxococcota and Actinomycetota in UNF soils and lower Acidobacteriota in RHF soils compared to AGR soils. Also, UNF had a lower abundance of Planctomycetota compared to RHF (Fig. 4A). A total of 40 bacterial taxa were differentially abundant across the disturbance gradient with eight distinct clusters (I-VIII) based on their similarities (Fig. 4B). In the dendrogram, Cluster I includes seven taxa ranging from the genus *Ellin6055* to the genus *IS-44*, which are more prevalent in RHF and UNF with varied abundance. This is followed by the smaller cluster II ranging from the family BSV26 to *Prolibacteraceae* with higher abundance in UNF. Cluster III comprises 12 taxa, from the family *Caulobacteraceae* to *Nannocystis*, which are more abundant in AGR soils. Cluster IV consists of taxa ranging from Burkholderiales to the genus *mle1-7* which are more abundant in RHF and UNF. In contrast, cluster V includes taxa from the family WD2101 soil group and *Haliangium*, both of which are more abundant in AGR. Clusters VI, VII, and VIII include taxa ranging from Alphaproteobacteria to NB1-j, class OM190 to family Comamonadaceae, and Microscillaceae to *Pseudomonas* respectively (Fig. 4B). These clusters are distinct with a differential abundance of taxa across the land uses.

Important features, indicator taxa, that differentiate these land uses were also identified using random forest classification. Key taxa identified were Burkholderiales, BSV26, and TRA3-20 in UNF; OM190, *Pseudomonas*, *Ellin605*, and CCM11a in RHF; and WD2101 soil group, *Rhodoplanes*, and *Haliangium* in AGR. (Fig. 4C). The indicator taxa were differentially abundant across land-use types and supported ALDEx2 analysis as shown in the heatmap (Fig. 4B).

3.5. Co-occurrence network patterns and topological properties

Bacterial co-occurrence patterns were explored using correlation-based networks constructed from cDNA sequencing data (Fig. 5A). The number of nodes in each co-occurring network did not differ significantly across the sites. The UNF network exhibited markedly higher connectivity, with 1269 edges, about twice the number of edges in AGR

(722) and RHF (607) (Fig. 5, Table S3). This heightened connectivity in UNF is further underscored by a smaller network diameter compared to RHF and AGR, suggesting shorter distances between the most distantly connected nodes. Likewise, a shorter average path length (APL=5.94) was observed in UNF compared to AGR (8.47) (Fig. 5B, Table S3). Furthermore, UNF presented a higher average degree, weighted degree, and average clustering coefficient compared to AGR and RHF (Fig. 5B, Table S3). The number of network modules or communities was greater in AGR (25) and RHF (23) compared to UNF (16) indicating higher community fragmentation under more disturbed conditions.

3.5.1. Network hubs

Microbial hubs, nodes with high eigenvector centrality (> 0.75), were identified as influential taxa within the network structure (Fig. 5A, Table 2). Eight hubs from three phyla, Actinomycetota (5 taxa), Bacillota, and Chloroflexota (2 taxa) were identified in AGR. Ten hubs, from five phyla, Acidobacteriota (2 taxa), Bacteroidota, Latescibacterota, Planctomycetota (2 taxa), and Pseudomonadota (4 taxa) were identified in RHF, and 12 hubs from 8 phyla Acidobacteriota, Chloroflexota, Desulfobacterota (3 taxa), Entotheonellaeota, Gemmatimonadota, Myxococcota, Nitrospirota, Pseudomonadota (3 taxa) were identified in UNF (Table 2). The taxa Micrococcaceae, *Lysobacter*, and TRA3-20 from AGR, RHF, and UNF, respectively, with the highest eigen centrality values, were the taxa with the most connections to other influential taxa. Based on rrn operon copy numbers, most hubs in AGR and RHF were classified as oligotrophs, with 1 or 2 taxa identified as intermediate strategists. While in UNF, two microbial hubs were classified as copiotrophs, including TRA3-20, the hub with the highest eigencentrality, and most influence in the network (Table 2). Links between microbial hubs, and soil resource availability across the land uses were explored through Spearman correlation analysis (Figure S3). Interestingly, microbial hubs from the AGR site were not correlated with any soil chemical properties, while the majority of the hubs from UNF were positively correlated with total soil carbon and nitrogen content, and 3 hubs were positively correlated with soil nitrate levels in RHF (Figure S3). These results follow a pattern of resource availability, where UNF had significantly higher Total C and N levels, and RHF had the

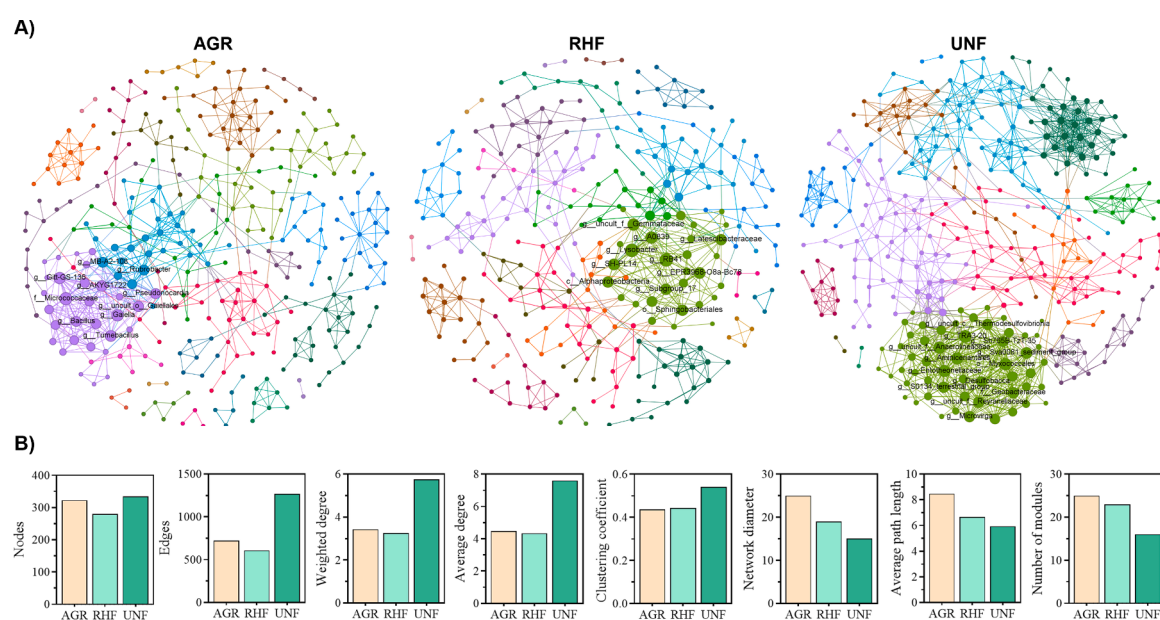


Fig. 5. (A) Bacterial co-occurrence networks from agricultural land (AGR), Rehabilitated Forest (RHF), and undisturbed natural forest (UNF). Bacterial nodes (taxa) and connecting edges (positive correlations) were calculated using SparCC ($P < 0.01, R > 0.75$). Nodes are colored according to their modularity class; nodes with the same color belong to the same module. Node size reflects eigenvector centrality, and labeled nodes are identified microbial hub taxa inferred based on their eigencentrality (> 0.75) (Listed in Table 2) (B) Bar plots showing differences between the topological parameters of co-occurrence networks of active bacterial communities in AGR, RHF, and UNF.

Table 2

Microbial hub taxa identified in agricultural land (AGR), rehabilitated agroforest buffer (RHF), and undisturbed natural forest (UNF). Ecological strategies were assigned based on rrn operon copy number: oligotrophs ($\text{rrn} \leq 2$), copiotrophs ($\text{rrn} \geq 5$), and intermediate strategists ($\text{rrn} = 3-4$).

Land Use	Microbial Hub	Phylum	Eigen centrality ^a	rRNA operon copies	Ecological Strategy ^b
AGR	Micrococcaceae	Actinomycetota	1	1	Oligotroph
	<i>Gaiella</i>	Actinomycetota	0.916	1	Oligotroph
	Gaiellales	Actinomycetota	0.798	1	Oligotroph
	<i>Pseudonocardia</i>	Actinomycetota	0.772	2	Oligotroph
	<i>MB-A2-108</i>	Actinomycetota	0.762	1	Oligotroph
	Gitt-GS-136	Chloroflexota	0.905	1	Oligotroph
	<i>AKYG1722</i>	Chloroflexota	0.828	2	Oligotroph
	<i>Tumebacillus</i>	Bacillota	0.837	3	Intermediate
	<i>Lysobacter</i>	Pseudomonadota	1	4	Intermediate
	<i>A0839</i>	Pseudomonadota	0.874	1	Oligotroph
RHF	<i>EPR3968-O8a-Bc78</i>	Pseudomonadota	0.797	1	Oligotroph
	Alphaproteobacteria	Pseudomonadota	0.761	2	Oligotroph
	<i>RB41</i>	Acidobacteriota	0.996	1	Oligotroph
	subgroup_17	Acidobacteriota	0.765	1	Oligotroph
	Gemmataceae	Planctomycetota	0.851	3	Intermediate
	<i>SH-PL14</i>	Planctomycetota	0.8	1	Oligotroph
	Latescibacteraceae	Latescibacterota	0.764	1	Oligotroph
	Sphingobacteriales	Bacteroidota	0.765	1	Oligotroph
	TRA3-20	Pseudomonadota	1	5	Copiotroph
	<i>Microvirga</i>	Pseudomonadota	0.822	1	Oligotroph
UNF	Reyranellaceae	Pseudomonadota	0.845	1	Oligotroph
	<i>Desulfobacula</i>	Desulfobacterota	0.752	1	Oligotroph
	Sva0081_sediment_group	Desulfobacterota	0.883	1	Copiotroph
	Geobacteraceae	Desulfobacterota	0.857	2	Oligotroph
	Myxococcales	Myxococcota	0.946	1	Oligotroph
	Anaerolineaceae	Chloroflexota	0.942	1	Oligotroph
	Aminicenatales	Acidobacteriota	0.934	1	Oligotroph
	Entotheonellaceae	Entotheonellaeota	0.917	1	Oligotroph
	S0134_terrestrial_group	Gemmatimonadota	0.841	10	Copiotroph
	Thermodesulfovibrio	Nitrospirota	0.795	1	Oligotroph

^a Hubs were defined as taxa with eigenvector centrality > 0.75 (Peschel et al., 2021). Eigenvector centrality measures a node's influence within a network.

^b Ecological strategies followed rrn thresholds adapted from Klappenbach et al. (2000).

highest soil Nitrate levels (Table 1).

Pairs of taxa with conserved co-occurrence associations across the three bacterial networks of the different land uses were also identified. We observed a small fraction (0.1 %) of associations conserved across AGR-RHF-UNF. These comprised two specific associations between Luteolibacter and TRA3-20 and Rokubacteriales and Gemmatimonadaceae (Figure S4). The numbers of shared associations between two land uses were: UNF-RHF, 18 associations (0.7 %); UNF-AGR, 20 associations (0.8 %); and AGR-RHF, 15 associations (0.6 %)

3.5.2. Network resilience

The network's robustness was explored using four removal strategies namely: random, betweenness centrality (BNC), degree-based, and cascading removal (Wang et al., 2023; Kratou et al., 2024; Abuin-Denis et al., 2024) (Fig. 6). Consistently, each of the strategies indicated that the AGR network was most vulnerable, requiring the removal of a smaller fraction of nodes to experience a 50 % loss in connectivity, highlighting its lower robustness compared to RHF and UNF networks (Fig. 6). The RHF network demonstrated moderate robustness, requiring more node removal than AGR but fewer than UNF to reach 50 % connectivity loss across most strategies. The UNF network was the most robust, requiring the greatest number of node removals under most attack strategies. However, under betweenness centrality (BNC) removal, RHF displayed similar resilience to UNF.

4. Discussion

Our findings show that disturbance alters the community structure of potentially active soil bacterial communities. The undisturbed natural forests supported more robust and interconnected microbial networks, while agricultural soils showed reduced resilience. The rehabilitated site

showed signs of partial recovery, indicating that long-term restoration can help reestablish functionally relevant microbial communities.

4.1. Edaphic drivers of microbial communities in rehabilitated and undisturbed forests were similar compared to agricultural sites

Three land uses were investigated in this study, with a clear disturbance gradient, including a disturbed conventional agricultural site (AGR) on a corn and soybean rotation, a previously disturbed rehabilitated agroforest (RHF) where rehabilitation began in 1985 and has now been undisturbed for over 33 years, and a natural forest that has remained undisturbed for over 150 years (UNF). The undisturbed and rehabilitated forest systems had the highest bacterial abundance (Fig. 2A) and were similar in community composition, sharing over 60 % of their ASVs (Fig. 2C, D). The higher moisture, nutrient contents, and lower temperature of these soils partially explained the difference in composition (Table 1, Fig. 3). Undisturbed forest systems have been shown to have enhanced soil nutrient levels and sequester more carbon due to the accumulation of organic matter from plant debris, leaf litter, and root exudates (Shen et al., 2024), these conditions are known to nurture higher bacterial populations and stimulate microbial activity (Lladó et al., 2017). In contrast, agricultural systems tend to be highly disturbed, and management practices such as tillage, annual crop rotation, and agro-chemical usage can impact soil conditions and drive changes in bacterial populations (Trivedi et al., 2016). In this system, the AGR site had higher soil bulk density and soil temperature, and lower soil carbon and nitrogen were associated with significantly lower bacterial abundance (16S genes and transcripts), and significantly different bacterial community composition, with 14 % of the ASVs being unique to the AGR site (Table 1, Fig. 2). Mean annual temperature and nutrient content, such as C:N ratios, are known drivers of the global

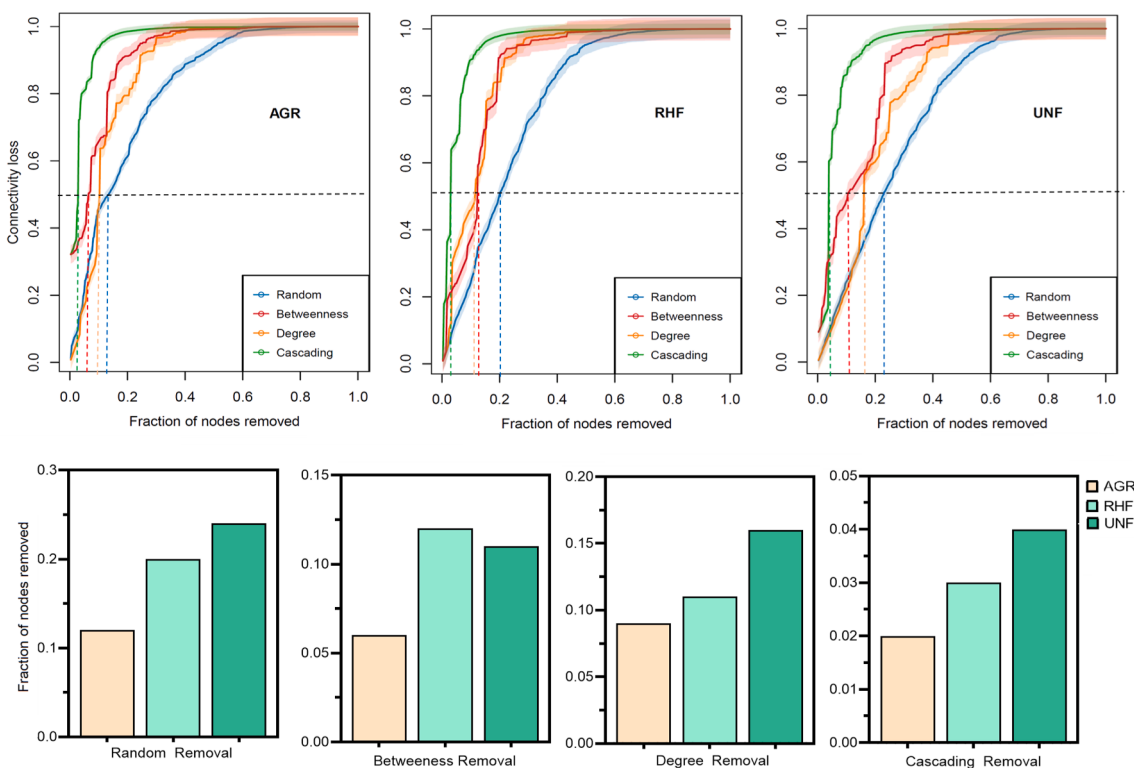


Fig. 6. Network robustness across AGR, RHF, UNF. Network tolerance to node removal was tested using different node removal strategies, in the order (from left to right): Cascading (green), Betweenness centrality (red), Degree (orange), and Random (blue). Loss of connectivity values ranges between 0 (maximum connectivity between nodes) to 1 (total disconnect between nodes). The proportion of nodes that made the network lose 0.50 connectivity for each attack strategy in AGR, RHF, and UNF is visualized with the broken lines. Bar plots show the fraction of nodes removed to achieve 50 % connectivity loss for four removal strategies.

topsoil microbiome (Bahram et al., 2018). While high bulk density associated with soil compaction may reduce pore space in the soil, limiting microbial habitats and potentially reducing bacterial abundance (Frene et al., 2024; Li et al., 2002), the AGR site had a bulk density in the normal range for agricultural soils. However, Jarrah et al. (2022) highlight that management practices like tillage and fertilizer application cause significant temporal variation in surface soil properties within agricultural systems. At the depths sampled in this study, within the plough layer, there could be temporary compaction due to seasonal applications of agrochemicals and planting or tillage. Solar radiation in these systems is also highly dynamic, leading to daily and seasonal fluctuations in soil temperatures, with higher temperatures in summer and colder in winter (Jarrah et al., 2022).

4.2. Rehabilitated forests shared more taxonomic similarities with undisturbed forests than with agricultural sites

Previously disturbed RHF soils showed an intermediate profile, with the relative abundance of most bacterial phyla being similar to that of the undisturbed UNF, and higher C, total N, and NH_4^+ than AGR (Table 1), suggesting a potential recovery trajectory. We observed that the distribution of dominant bacterial phyla differed with land use. Pseudomonadota was the most common bacterial phylum in all soils and showed substantial variation in abundance, ranging from over 34 % in the forest soils (RHF and UNF) to 26 % in the AGR soils. The higher abundance of Pseudomonadota in the forest soils compared to AGR is consistent with a previous study by Trivedi et al. (2016), which found a higher abundance of Pseudomonadota in natural soils compared to agricultural soils across all their studied regions. In the undisturbed UNF, key taxa such as Burkholderiales (cluster IV) and TRA3–20 (cluster VII), both belonging to Pseudomonadota, known for their roles in pathogen suppression and carbon mineralization (Aguirre-von-Wobeser, et al., 2018; Xiao et al., 2022), were identified by random forest analysis

as key indicator taxa that differentiate between sites. Both groups are known for their adaptability in maintaining soil health and promoting plant resilience, making them key indicators of a fertile and biologically robust ecosystem.

The significantly higher soil pH in the previously disturbed RHF was the likely driver of a lower abundance of Acidobacteriota compared to AGR and UNF. While some subgroups of Acidobacteriota are acidophilic and tend to dominate in low-pH soils, others prefer neutral to alkaline conditions. Therefore, shifts in the relative abundance of Acidobacteriota across sites may reflect the differential pH preferences of specific subgroups (Conradie and Jacobs, 2021; Röttjers and Faust, 2018).

In the rehabilitated forest (RHF), random forest analysis identified *Ellin6055* and *Pseudomonas* from the phylum Pseudomonadota, corresponding to clusters I and VIII, respectively as key indicator taxa. Similarly, the phylum Planctomycetota was most abundant in RHF, with key taxa such as CCM11a and OM190, from clusters IV and VII, as indicator taxa that differentiate these land uses (Fig. 4). These gram-negative organisms are often linked to plant growth and rooting systems (Yasmeen et al., 2021; Sah et al., 2021; Mafa-Attaye et al., 2023), suggesting their presence could indicate enhanced plant growth and restoration processes in rehabilitated agroforestry systems. The AGR soils had a higher abundance of Actinomycetota (Fig. 4A), (Trivedi et al., 2016), a group characterized by high resistance to moisture stress because of their thick cell walls and spore formation (Yang et al., 2024; Bhatti et al., 2017). Gram-positive bacteria and actinomycetes have recently been shown to dominate when temperatures fluctuate and in wet-dry cycles (Yang et al., 2024), and nitrogen fertilization may have increased the relative abundance of Actinomycetota (Dai et al., 2018). Also, the phylum Acidobacteriota was more abundant in AGR soils. A study by Navarrete et al. (2013) showed that Acidobacteriota subgroups 4, 6, and 7 were more abundant in cropland and could serve as early indicators of the impact of agricultural practices on soil health,

responding notably to shifts in pH, aluminum, calcium, and magnesium levels. Key bacterial taxa differentiating the AGR site included *Halianium* (Myxococcota) which plays a crucial role in these restoration processes by contributing to soil biogeochemical cycles (Hu et al., 2022) and crucial for enhancing soil health. We also identified WD2101 soil group (Plantomycetota), within cluster V as a key taxon. Previous studies have highlighted this group's essential role in enhancing soil multifunctionality across ecosystems (Dedysh et al., 2021; Delgado-Baquerizo et al., 2017).

4.3. Robustness of co-occurrence networks decreased with disturbance

The structure of co-occurrence networks provided exploratory insights into taxon association patterns within microbial communities across the different gradients. The network structure in UNF showed greater connectivity, and a higher average clustering coefficient, combined with a smaller network diameter and shorter average path length compared to RHF and AGR. These topological features suggest a more tightly connected community structure in UNF. This efficient microbial community structure probably promotes effective interaction among species (Kim et al., 2019). Although RHF had fewer nodes and edges compared to AGR, its higher average clustering coefficient, smaller network diameter, and shorter path length suggest stronger co-occurrence among taxa in RHF.

Several microbial hubs, or highly connected taxa in the network, differed across the different land uses. These taxa are influential within the co-occurrence network, and may maintain the structure of microbial communities (Banerjee et al., 2019; Rottjers and Faust, 2018). Availability of resources can partially be responsible for co-occurrence of taxa, where the nutritional requirements of organisms favour particular environments (Banerjee et al., 2016). Microbial ecological strategies have been classified into an oligotroph – copiotroph continuum. Oligotrophs are adapted to resist environmental stress, and typically have higher carbon use efficiency, and few rRNA operon (*rrn*) copies in their genome, while copiotrophs have rapid growth in resource-rich conditions, and higher *rrn* copy numbers (Fierer et al., 2007; Klappenbach et al., 2000). In our study, the community weighted mean *rrn* copy number indicated that all soils were dominated by oligotrophic taxa, with AGR soils having the lowest number of copiotrophs (Table S2). While Stone et al. (2023) also found that the majority of ASVs in aerobic, mineral soils are classified as oligotrophs they caution the categorization of organisms into ecological categories at broader taxonomic resolution, since many taxa fall within the continuum of the two categories depending on soil characteristics, nutrient availability and local biotic interactions rather than genome size. The predominant hubs in AGR were mainly from the phylum Actinomyceota whereas both the forest soils were dominated by hubs from the phylum Pseudomonadota (Table 2). Karimi et al. (2019), also found Actinomyceota as hub taxa in agricultural soils and reported a shift in the microbial hubs from oligotrophs in agricultural soils, where organic carbon and nitrogen contents were the lowest, to copiotrophic taxa that dominate in nutrient-rich forest soils. Similarly, soil resources shifted across the disturbance gradient in our system, where the lowest soil carbon and nitrogen levels were quantified in AGR (Table 1). AGR hubs, such as *Micrococcaceae* and *Pseudonocardia*, were predominantly oligotrophic (*rrn* \leq 2) and had traits that indicate environmental stress resistance, such as the degradation of recalcitrant organic compounds. No significant correlations existed between AGR hubs and soil nutrient variables (Figure S3), suggesting limited responsiveness to resource availability and stress-tolerant microbes with the capacity to metabolize low-quality organic matter (Chen et al., 2018; Storey et al., 2018).

In RHF, two of the hubs, *RB41* and *Lysobacter* were positively correlated with soil nitrate concentrations (Figure S3). *RB41* is known to play roles in nitrogen cycling, plant growth promotion, and carbon sequestration (Duan et al., 2021; Fu et al., 2021), while *Lysobacter* is known for its biocontrol properties, contributes to disease suppression

(Gómez Expósito et al., 2015; Vlassi et al., 2020). This suggests that these taxa are functionally responsive, and restoration efforts may have re-established taxa capable of mediating key ecosystem processes.

In UNF, the hub taxa included *TRA3–20*, a copiotroph, which plays a role in carbon mineralization (Xiao et al., 2022), and *Microvirga* (oligotroph), a nitrogen-fixing genus known to harbor *nifH* genes (Radl et al., 2014). This ecological role aligns with previous studies at the same site, which reported significantly higher *nifH* gene abundances in UNF soils compared to agricultural fields (Mafa-Attoye et al., 2020). Most hubs in UNF were strongly and positively correlated with soil carbon, nitrogen, and moisture content, supporting the view that resource-driven network assembly occurs under high organic matter availability (Table 1, Figure S3, Banerjee et al., 2016). Banerjee et al. (2016) also showed that more connected and functionally diverse hub taxa contribute to ecosystem stability and multifunctionality under less-disturbed conditions.

Across the three bacterial networks, a small number of co-occurrence associations were conserved across all three networks, *Luteolibacter* with *TRA3–20*, and *Rokubacteriales* with *Gemmataimonadaceae*. These conserved associations suggest that these taxa are functionally interdependent and may reflect shared environmental responses or possible stability in community structure across diverse land uses (Becraft et al., 2017).

Highly connected networks typically exhibit greater stability due to their buffering capacity (Yu et al., 2022; Landi et al., 2018). The AGR network was the most vulnerable and least robust of all the networks requiring the removal of fewer nodes to reach the 50 % connectivity loss threshold. This reduced robustness in AGR is likely due to agricultural intensification, which reduces bacterial network complexity (Banerjee et al., 2019; Karimi et al., 2019; Lan et al., 2022). The high number of modules in AGR could indicate a higher degree of ecological niches or specialization within the microbial community (Ma et al., 2020). This could be a consequence of varying environmental pressures and management practices and an indicator of a diverse range of functional groups adapted to the varying conditions created by agricultural practices (Banerjee et al., 2019). However, the higher number of modules can also indicate that the network is less robust, as impacts on one module might not easily be compensated for by others, potentially making the network more susceptible to environmental stresses (Hernandez et al., 2021).

In contrast, the UNF network was more resilient than AGR and RHF, as it required the removal of a larger fraction of nodes to achieve the same level of connectivity loss. This suggests that UNF has a more complex structure, with a higher number of redundant links allowing for better absorption of shocks without substantial loss of function. The lower number of modules in UNF possibly reflects a more integrated microbial community, with redundant functions across different species, contributing to its resilience (Tian et al., 2020). This resilience is crucial in undisturbed environments, where species rely on natural processes to maintain ecosystem stability (Wang et al., 2023). The RHF network exhibits moderate robustness, requiring more node removals than AGR but fewer than UNF to reach 50 % connectivity loss across most strategies. This reflects its partially restored structure following rehabilitation over 33 years ago. While its resilience to random and degree-based attacks indicates that the network has developed a more interconnected form, the comparable performance to UNF under betweenness centrality (BNC) removal suggests that critical nodes still play a significant role in maintaining overall network connectivity. Although it remains less robust than UNF, this may reflect a semi-natural habitat that experiences some human influence and is progressively being restored toward a more natural state, indicative of ongoing ecological restoration (Atkinson et al., 2022).

While our study provides new insights into the structure and resilience of potentially active soil microbial communities across a disturbance gradient, it has some limitations.

As earlier noted, the land-use types represent single, long-established

sites rather than replicated experimental units. This limits the applicability of the results and introduces the possibility that some observed microbial differences may reflect site-specific factors unrelated to disturbance. Also, this study focused on the potentially active fraction of the microbial community. Future work that integrates both DNA- and RNA-based microbial profiling could provide deeper insights into how total and active communities respond to long-term ecological restoration. Such comparisons would enable researchers to explore functional redundancy, dormancy dynamics, and the persistence of microbial taxa across disturbance gradients.

5. Conclusion

Our findings show that disturbances significantly impact soil properties and microbial community structure. Bacterial co-occurrence networks and resilience varied according to the degree of disturbance in each land use, supporting the hypothesis that less disturbed soils will have greater connectivity. The undisturbed natural forest maintained a more complex and robust microbial network compared to the rehabilitated and agricultural lands. This highlights the importance of conserving natural forest ecosystems to enhance soil health and ecosystem functions. RHF exhibits characteristics that are intermediate between AGR and UNF, suggesting a long-term transition that could be leveraged in rehabilitation efforts potentially spanning over 30 years. Our findings contribute valuable insights into how disturbances influence soil microbial community structure and co-occurrence patterns.

CRediT authorship contribution statement

Tolulope G. Mafa-Attoye: Writing – original draft, Visualization, Methodology, Formal analysis, Data curation, Conceptualization. **Daniel Obregon:** Writing – review & editing, Visualization, Methodology, Formal analysis. **Micaela Tosi:** Writing – review & editing, Visualization, Formal analysis. **Maren Oelbermann:** Writing – review & editing, Conceptualization. **Naresh V. Thevathasan:** Writing – review & editing, Funding acquisition, Conceptualization. **Kari E. Dunfield:** Writing – review & editing, Supervision, Project administration, Funding acquisition, Conceptualization.

Declaration of Competing Interest

The authors declare that they have no known competing financial interests or personal relationships that could have appeared to influence the work reported in this paper.

Acknowledgments

We extend our gratitude to Brian and Elizabeth Tew, Josie and Jens Madsen, and other landowners for granting access to their land and the Grand River Conservation Authority for their assistance with identifying research sites. We are grateful to Kira A. Borden for providing laboratory analysis data on total C and total N. We also appreciate the technical support provided by Kamini Khosla. This research was financially supported by the Agriculture and AgriFood Canada, Agricultural Greenhouse Gas Program (AGGP), Canada First Research Excellence Fund (CFREF) (Food from Thought) and an NSERC Discovery Grant (Dunfield, RGPIN 2019-05005).

Appendix A. Supporting information

Supplementary data associated with this article can be found in the online version at [doi:10.1016/j.agee.2025.109813](https://doi.org/10.1016/j.agee.2025.109813).

Data availability

Data will be made available on request.

References

- Abuin-Denis, L., Piloto-Sardiñas, E., Maitre, A., Wu-Chuang, A., Mateos-Hernández, L., Paulino, P.G., Bello, Y., Bravo, F.L., Gutierrez, A.A., Fernández, R.R., Castillo, A.F., 2024. Differential nested patterns of Anaplasma marginale and Coxiella-like endosymbionts across Rhinocerophalus microplus ontogeny. *Microbiol. Res.*, 127790. <https://doi.org/10.1016/j.micres.2024.127790>.
- Aguirre-von-Wobeser, E., Rocha-Estrada, J., Shapiro, L.R., de la Torre, M., 2018. Enrichment of Verrucomicrobia, Actinobacteria and Burkholderiales drives selection of bacterial community from soil by maize roots in a traditional milpa agroecosystem, 10.1371/journal.pone.0208852 PLoS One 13 (12), e0208852. <https://doi.org/10.1371/journal.pone.0208852>.
- Aitchison, J., 1986. *The Statistical Analysis of Compositional Data*. Reprinted in 2003 with additional material by The Blackburn Press, Chapman & Hall: London.
- Allison, S.D., Martiny, J.B., 2008. Resistance, resilience, and redundancy in microbial communities. *Proc. Natl. Acad. Sci.* 105 (ement_1), 11512–11519. <https://doi.org/10.1073/pnas.0801925105>.
- Apprill, A., McNally, S., Parsons, R., Weber, L., 2015. Minor revision to V4 region SSU rRNA 806R gene primer greatly increases detection of SAR11 bacterioplankton. *Aquat. Microb. Ecol.* 75 (2), 129–137. <https://doi.org/10.3354/ame01753>.
- Atkinson, J., Brudvig, L.A., Mallen-Cooper, M., Nakagawa, S., Moles, A.T., Bonser, S.P., 2022. Terrestrial ecosystem restoration increases biodiversity and reduces its variability, but not to reference levels: a global meta-analysis. *Ecol. Lett.* 25 (7), 1725–1737. <https://doi.org/10.1111/ele.14025>.
- Bahram, M., Hildebrand, F., Forslund, S.K., Anderson, J.L., Soudzilovskaya, N.A., Bodegom, P.M., Bengtsson-Palme, J., Ansari, S., Coelho, L.P., Harend, H., Huerta-Cepas, J., 2018. Structure and function of the global topsoil microbiome. *Nature* 560 (7717), 233–237. <https://doi.org/10.1038/s41586-018-0386-6>.
- Baldrian, P., Kolarík, M., Stursová, M., Kopecký, J., Valášková, V., Větrovský, T., Žiřćáková, L., Šnajdr, J., Rídl, J., Vlček, Č., Voršíková, J., 2012. Active and total microbial communities in forest soil are largely different and highly stratified during decomposition. *ISME J.* 6 (2), 248–258.
- Banerjee, S., Kirkby, C.A., Schmutz, D., Bissett, A., Kirkegaard, J.A., Richardson, A.E., 2016. Network analysis reveals functional redundancy and keystone taxa amongst bacterial and fungal communities during organic matter decomposition in an arable soil. *Soil Biol. Biochem.* 97, 188–198.
- Banerjee, S., Walder, F., Büchi, L., Meyer, M., Held, A.Y., Gattinger, A., Keller, T., Charles, R., van der Heijden, M.G., 2019. Agricultural intensification reduces microbial network complexity and the abundance of keystone taxa in roots. *ISME J.* 13 (7), 1722–1736. <https://doi.org/10.1038/s41396-019-0383-2>.
- Bastian, M., Heymann, S., Jacomy, M., 2009. Gephi: an open source software for exploring and manipulating networks. *Proc. Int. AAAI Conf. Web Soc. Media* 3 (1), 361–362. <https://doi.org/10.1609/icwsm.v3i1.13937>.
- Becraft, E.D., Woyke, T., Jarett, J., Ivanova, N., Godoy-Vitorino, F., Poulton, N., Brown, J.M., Brown, J., Lau, M.C., Onstott, T., Eisen, J.A., 2017. Rokubacteria: genomic giants among the uncultured bacterial phyla. *Front. Microbiol.* 8, 2264. <https://doi.org/10.3389/fmicb.2017.02264>.
- Bhatti, A.A., Haq, S., Bhat, R.A., 2017. Actinomycetes benefaction role in soil and plant health. *Microb. Pathog.* 111, 458–467. <https://doi.org/10.1016/j.micpath.2017.09.036>.
- Blazewicz, S.J., Barnard, R.L., Daly, R.A., Firestone, M.K., 2013. Evaluating rRNA as an indicator of microbial activity in environmental communities: limitations and uses. *ISME J.* 7, 2061–2068. <https://doi.org/10.1038/ismej.2013.102>.
- Bokulich, N.A., Kaebler, B.D., Rideout, J.R., Dillon, M., Bolyen, E., Knight, R., Huttley, G.A., Caporaso, J.G., 2018. Optimizing taxonomic classification of marker-gene amplicon sequences with QIIME 2's q2-feature-classifier plugin. *Microbiome* 6 (1), 1–17. <https://doi.org/10.1186/s40168-018-0470-z>.
- Bolyen, E., Rideout, J.R., Dillon, M.R., Bokulich, N.A., Abnet, C.C., Al-Ghalith, G.A., Alexander, H., Alm, E.J., Arumugam, M., Asnicar, F., Bai, Y., Bisanz, J.E., Bittinger, K., Brejnrod, A., Brislawn, C.J., Brown, C.T., Callahan, B.J., Caraballo-Rodríguez, A.M., Chase, J., Cope, E.K., Da Silva, R., Diener, C., Dorrestein, P.C., Douglas, G.M., Durall, D.M., Duvallet, C., Edwardson, C.F., Ernst, M., Estaki, M., Fouquier, J., Gauglitz, J.M., Gibbons, S.M., Gibson, D.L., Gonzalez, A., Gorlick, K., Guo, J., Hillmann, B., Holmes, S., Holste, H., Huttenhower, C., Huttley, G.A., Janssen, S., Jarmusch, A.K., Jiang, L., Kaebler, B.D., Kang, K.B., Keeffe, C.R., Keim, P., Kelley, S.T., Knights, D., Koester, I., Kosciolék, T., Kreps, J., Langille, M.G., Lee, J., Ley, R., Liu, Y.X., Loftfield, E., Lozupone, C., Maher, M., Marotz, C., Martin, B.D., McDonald, D., McIver, L.J., Melnik, A.V., Metcalf, J.L., Morgan, S.C., Morton, J.T., Naimey, A.T., Navas-Molina, J.A., Nothias, L.F., Orchanian, S.B., Pearson, T., Peoples, S.L., Petras, D., Preuss, M.L., Pruesse, E., Rasmussen, L.B., Rivers, A., Robeson, M.S., Rosenthal, P., Segata, N., Shaffer, M., Shiffer, A., Sinha, R., Song, S.J., Spear, J.R., Swafford, A.D., Thompson, L.R., Torres, P.J., Trinh, P., Tripathi, A., Turnbaugh, P.J., Ul-Hasan, S., 2019. Reproducible, interactive, scalable and extensible microbiome data science using QIIME 2. *Nat. Biotechnol.* 37, 852–857. <https://doi.org/10.1038/s41587-019-0209-9>.
- Borden, K.A., Mafa-Attoye, T.G., Dunfield, K.E., Thevathasan, N.V., Gordon, A.M., Isaac, M.E., 2021. Root functional trait and soil microbial coordination: implications for soil respiration in riparian agroecosystems. *Front. Plant Sci.* 12, 681113. <https://doi.org/10.3389/fpls.2021.681113>.
- Callahan, B.J., McMurdie, P.J., Rosen, M.J., Han, A.W., Johnson, A.J.A., Holmes, S.P., 2016. DADA2: High-resolution sample inference from Illumina amplicon data. *Nat. Methods* 13 (7), 581–583. <https://doi.org/10.1038/nmeth.3869>.
- Chen, S.C., Duan, G.L., Ding, K., Huang, F.Y., Zhu, Y.G., 2018. DNA stable-isotope probing identifies uncultivated members of *Pseudonocardia* associated with biodegradation of pyrene in agricultural soil. *FEMS Microbiol. Ecol.* 94 (3) p.fiy026.

- Chong, J., Liu, P., Zhou, G., Xia, J., 2020. Using MicrobiomeAnalyst for comprehensive statistical, functional, and meta-analysis of microbiome data. *Nat. Protoc.* 15 (3), 799–821. <https://doi.org/10.1038/s41596-019-0264-1>.
- Conradie, T.A., Jacobs, K., 2021. Distribution patterns of Acidobacteriota in different fynbos soils. *PLoS One* 16 (3), e0248913. <https://doi.org/10.1371/journal.pone.0248913>.
- Core Team, R., 2020. R: A Language and Environment for Statistical Computing. R Foundation for Statistical Computing, Vienna. Available at: (<https://www.R-project.org/>).
- Csardi, G., Nepusz, T., 2006. The igraph software package for complex network research. *Inter. Complex Syst.* 1695, 1–9.
- Dai, Z., Su, W., Chen, H., Barberán, A., Zhao, H., Yu, M., Yu, L., Brookes, P.C., Schadt, C. W., Chang, S.X., Xu, J., 2018. Long-term nitrogen fertilization decreases bacterial diversity and favors the growth of Actinobacteria and Proteobacteria in agro-ecosystems across the globe. *Glob. Chang Biol.* 24 (8), 3452–3461. <https://doi.org/10.1111/gcb.14163>.
- De Carlo, N.D., Oelbermann, M., Gordon, A.M., 2019. Spatial and temporal variation in soil nitrous oxide emissions from a rehabilitated and undisturbed riparian forest. *J. Environ. Qual.* 48 (3), 624–633. <https://doi.org/10.2134/jeq2018.09.0346>.
- Dedysh, S.N., Beletsky, A.V., Ivanova, A.A., Kulichevskaya, I.S., Suzina, N.E., Philippov, D.A., Rakitin, A.L., Mardanov, A.V., Ravin, N.V., 2021. Wide distribution of Phycisphaera-like planctomycetes from WD2101 soil group in peatlands and genome analysis of the first cultivated representative. *Environ. Microbiol.* 23 (3), 1510–1526. <https://doi.org/10.1111/1462-2920.15360>.
- Delgado-Baquerizo, M., Eldridge, D.J., Ochoa, V., Gozalo, B., Singh, B.K., Maestre, F.T., 2017. Soil microbial communities drive the resistance of ecosystem multifunctionality to global change in drylands across the globe. *Ecol. Lett.* 20 (10), 1295–1305. <https://doi.org/10.1111/ele.12826>.
- Douglas, G.M., Maffei, V.J., Zaneveld, J., Yurgel, S.N., Brown, J.R., Taylor, C.M., Huttenthaler, C., Langille, M.G.I., 2020. PICRUSt2: an improved and extensible approach for metagenome inference. *Nat. Biotechnol.* 38 (6), 685–688. <https://doi.org/10.1038/s41587-020-0548-6>.
- Duan, R., Lin, Y., Zhang, J., Huang, M., Du, Y., Yang, L., Bai, J., Xiang, G., Wang, Z., Zhang, Y., 2021. Changes in diversity and composition of rhizosphere bacterial community during natural restoration stages in antimony mine. *PeerJ* 9, e12302. <https://doi.org/10.7717/peerj.12302>.
- Environment and Climate Change Canada, 2020. Canadian climate normals 1981–2010. Station Data.
- Faust, K., Raes, J., 2012. Microbial interactions: from networks to models. *Nat. Rev. Microbiol.* 10 (8), 538–550. <https://doi.org/10.1038/nrmicro2832>.
- Fierer, N., Bradford, M.A., Jackson, R.B., 2007. Toward an ecological classification of soil bacteria. *Ecology* 88 (6), 1354–1364.
- Fierer, N., Jackson, J.A., Vilgalys, R., Jackson, R.B., 2005. Assessment of soil microbial community structure by use of taxon-specific quantitative PCR assays. *Appl. Environ. Microbiol.* 71 (7), 4117–4120. <https://doi.org/10.1128/AEM.71.7.4117-4120.2005>.
- Frene, J.P., Pandey, B.K., Castrillo, G., 2024. Under pressure: elucidating soil compaction and its effect on soil functions. *Plant Soil* 502 (1), 267–278.
- Friedman, J. and Alm, E.J., 2012. Inferring correlation networks from genomic survey data. DOI: [10.1371/journal.pcbi.1002687](https://doi.org/10.1371/journal.pcbi.1002687).
- Fu, Y., Kumar, A., Chen, L., Jiang, Y., Ling, N., Wang, R., Pan, Q., Singh, B.P., Redmile-Gordon, M., Luan, L., Li, Q., 2021. Rhizosphere microbiome modulated effects of biochar on ryegrass 15 N uptake and rhizodeposited 13C allocation in soil. *Plant Soil* 463, 359–377. <https://doi.org/10.1007/s11104-021-04940-2>.
- Gloor, G.B., Macklaim, J.M., Fernandes, A.D., 2016. Displaying variation in large datasets: plotting a visual summary of effect sizes. *J. Comput. Graph. Stat.* 25 (3), 971–979. <https://doi.org/10.1080/10618600.2015.1131161>.
- Gómez Expósito, R., Postma, J., Raaijmakers, J.M., De Bruijn, I., 2015. Diversity and activity of Lysobacter species from disease suppressive soils. *Front. Microbiol.* 6, 1243. <https://doi.org/10.3389/fmicb.2015.01243>.
- Graziano, M.P., Deguire, A.K., Surasinghe, T.D., 2022. Riparian buffers as a critical landscape feature: insights for riverscape conservation and policy renovations. *Diversity* 14 (3), 172. <https://doi.org/10.3390/di14030172>.
- Hernandez, D.J., David, A.S., Menges, E.S., Searcy, C.A., Afkhami, M.E., 2021. Environmental stress destabilizes microbial networks. *ISME J.* 15 (6), 1722–1734. <https://doi.org/10.1038/s41396-021-00899-7>.
- Ho, A., Van den Brink, E., Reim, A., Krause, S.M., Bodelier, P.L., 2016. Recurrence and frequency of disturbance have cumulative effect on methanotrophic activity, abundance, and community structure. *Front. Microbiol.* 6, 1493. <https://doi.org/10.3389/fmicb.2015.01493>.
- Hu, L., Li, Q., Yan, J., Liu, C., Zhong, J., 2022. Vegetation restoration facilitates belowground microbial network complexity and recalcitrant soil organic carbon storage in southwest China karst region. *Sci. Total Environ.* 820, 153137. <https://doi.org/10.1016/j.scitotenv.2022.153137>.
- Hundal, H., Thevathasan, N.V., Oelbermann, M., 2024. Riparian vegetation influences aquatic greenhouse gas production in an agricultural landscape. *Ecol. Eng.* 208, 107386. <https://doi.org/10.1016/j.ecoleng.2023.107386>.
- Hutchins, D.A., Jansson, J.K., Remais, J.V., Rich, V.I., Singh, B.K., Trivedi, P., 2019. Climate change microbiology—problems and perspectives. *Nat. Rev. Microbiol.* 17 (6), 391–396. <https://doi.org/10.1038/s41579-019-0178-5>.
- Jarrahd, M., Mayel, S., Franko, U., Kukka, K., 2022. Effects of agricultural management practices on the temporal variability of soil temperature under different crop rotations in Bad Lauchstaedt-Germany. *Agronomy* 12 (5), 1199. <https://doi.org/10.3390/agronomy12051199>.
- Karimi, B., Dequiedt, S., Terrat, S., Jolivet, C., Arrouays, D., Wincker, P., Cruaud, C., Bispo, A., Chemidlin Prévost-Bouré, N., Ranjard, L., 2019. Biogeography of soil bacterial networks along a gradient of cropping intensity. *Sci. Rep.* 9 (1), 3812. <https://doi.org/10.1038/s41598-019-40339-2>.
- Karimi, B., Maron, P.A., Chemidlin-Prevost Bouré, N., Bernard, N., Gilbert, D., Ranjard, L., 2017. Microbial diversity and ecological networks as indicators of environmental quality. *Environ. Chem. Lett.* 15, 265–281. <https://doi.org/10.1007/s10311-017-0614-6>.
- Kim, E.Y., Ashlock, D., Yoon, S.H., 2019. Identification of critical connectors in the directed reaction-centric graphs of microbial metabolic networks. *BMC Bioinforma.* 20, 1–13. <https://doi.org/10.1186/s12859-019-2897-z>.
- Klappenbach, J.A., Dunbar, J.M., Schmidt, T.M., 2000. rRNA operon copy number reflects ecological strategies of bacteria. *Appl. Environ. Microbiol.* 66 (4), 1328–1333.
- Kratou, M., Maitre, A., Abuin-Denis, L., Piloto-Sardiñas, E., Corona-Guerrero, I., Cano-Angüelles, A.L., Wu-Chuang, A., Bamgbose, T., Almazan, C., Mosqueda, J., Obregón, D., 2024. Disruption of bacterial interactions and community assembly in Babesia-infected Haemaphysalis longicornis following antibiotic treatment. *BMC Microbiol.* 24 (1), 322. <https://doi.org/10.1186/s12866-024-03468-1>.
- Lan, G., Yang, C., Wu, Z., Sun, R., Chen, B., Zhang, X., 2022. Network complexity of rubber plantations is lower than tropical forests for soil bacteria but not for fungi. *Soil* 8 (1), 149–161. <https://doi.org/10.5194/soil-8-149-2022>.
- Landi, P., Minoarivelho, H.O., Bränström, Å., Hui, C., Dieckmann, U., 2018. Complexity and stability of ecological networks: a review of the theory. *Popul. Ecol.* 60 (4), 319–345. <https://doi.org/10.1007/s10144-018-0628-3>.
- Lee, K.K., Kim, H., Lee, Y.H., 2022. Cross-kingdom co-occurrence networks in the plant microbiome: importance and ecological interpretations. *Front. Microbiol.* 13, 953300.
- Legendre, P., Anderson, M.J., 1999. Distance-based redundancy analysis: testing multispecies responses in multifactorial ecological experiments. *Ecol. Monogr.* 69 (1), 1–24.
- Li, C.H., Ma, B.L., Zhang, T.Q., 2002. Soil bulk density effects on soil microbial populations and enzyme activities during the growth of maize (*Zea mays* L.) planted in large pots under field exposure. *Can. J. Soil Sci.* 82 (2), 147–154. <https://doi.org/10.4141/S01-026>.
- Liaw, A., Wiener, M., 2002. Classification and regression by randomForest. *R. N.* 2 (3), 18–22.
- Lind, L., Hasselquist, E.M., Laudon, H., 2019. Towards ecologically functional riparian zones: a meta-analysis to develop guidelines for protecting ecosystem functions and biodiversity in agricultural landscapes. *J. Environ. Manag.* 249, 109391. <https://doi.org/10.1016/j.jenvman.2019.109391>.
- Lladó, S., López-Mondejar, R., Baldrian, P., 2017. Forest soil bacteria: diversity, involvement in ecosystem processes, and response to global change. *Microbiol. Mol. Biol. Rev.* 81 (2), 10–128. <https://doi.org/10.1128/mmbr.00063-16>.
- Ma, B., Wang, Y., Ye, S., Liu, S., Stirling, E., Gilbert, J.A., Faust, K., Knight, R., Jansson, J. K., Cardona, C., Röttgers, L., 2020. Earth microbial co-occurrence network reveals interconnection pattern across microbiomes. *Microbiome* 8, 1–12. <https://doi.org/10.1186/s40168-020-00857-2>.
- Mafa-Attaye, T.G., Baskerville, M.A., Ofosu, E., Oelbermann, M., Thevathasan, N.V., Dunfield, K.E., 2020. Riparian land-use systems impact soil microbial communities and nitrous oxide emissions in an agro-ecosystem. *Sci. Total Environ.* 724, 138148. <https://doi.org/10.1016/j.scitotenv.2020.138148>.
- Mafa-Attaye, T.G., Borden, K.A., Alvarez, D.O., Thevathasan, N., Isaac, M.E., Dunfield, K. E., 2023. Roots alter soil microbial diversity and interkingdom interactions in diversified agricultural landscapes. *Oikos* 2023 (1). <https://doi.org/10.1111/oik.08717>.
- Miranda, K.M., Esprey, M.G., Wink, D.A., 2001. A rapid, simple spectrophotometric method for simultaneous detection of nitrate and nitrite. *Nitric Oxide* 5 (1), 62–71. <https://doi.org/10.1006/niox.2000.0319>.
- Mozuraitis, E. and Hagarty, J., 1996. Upgrade of soil survey information for Oxford County.
- Navarrete, A.A., Kuramae, E.E., de Hollander, M., Pijl, A.S., van Veen, J.A., Tsai, S.M., 2013. Acidobacterial community responses to agricultural management of soybean in Amazon forest soils. *FEMS Microbiol. Ecol.* 83 (3), 607–621. <https://doi.org/10.1111/1574-6941.12018>.
- Nemergut, D.R., Knelman, J.E., Ferrenberg, S., Bilinski, T., Melbourne, B., Jiang, L., Violette, C., Darcy, J.L., Prest, T., Schmidt, S.K., Townsend, A.R., 2016. Decreases in average bacterial community rRNA operon copy number during succession. *ISME J.* 10 (5), 1147–1156.
- Oelbermann, M., Gordon, A.M., Kaushik, N.K., 2008. Biophysical changes resulting from 16 years of riparian forest rehabilitation: an example from the Southern Ontario agricultural landscape. *Agrofor. Des. Ecol. Approach* 13–26.
- Oelbermann, M. and Gordon, A.M., 2000. Quantity and quality of autumnal litterfall into a rehabilitated agricultural stream (Vol. 29, No. 2, pp. 603–611). American Society of Agronomy, Crop Science Society of America, and Soil Science Society of America.
- Oelbermann, M., Raimbault, B.A., Gordon, A.M., 2015. Erratum to: Riparian Land-Use and Rehabilitation: Impact on Organic Matter Input and Soil Respiration. *Environ. Manag.* 56, 569. <https://doi.org/10.1007/s00267-015-0540-y>.
- Oelbermann, M., Raimbault, B.A., 2015. Riparian land-use and rehabilitation: Impact on organic matter input and soil respiration. *Environ. Manag.* 55, 496–507. <https://doi.org/10.1007/s00267-014-0410-z>.
- Oliveros, J.C., 2015. VENNY. An interactive tool for comparing lists with Venn Diagrams. (<http://bioinfogp.cnb.csic.es/tools/venny/index.html>).
- Parada, A.E., Needham, D.M., Fuhrman, J.A., 2016. Every base matters: assessing small subunit rRNA primers for marine microbiomes with mock communities, time series and global field samples. *Environ. Microbiol.* 18 (5), 1403–1414. <https://doi.org/10.1111/1462-2920.13023>.

- Peschel, S., Müller, C.L., Von Mutius, E., Boulesteix, A.L., Depner, M., 2021. NetCoMi: network construction and comparison for microbiome data in R. *Brief. Bioinforma.* 22 (4), bbaa290. <https://doi.org/10.1093/bib/bbaa290>.
- Philipott, L., Griffiths, B.S., Langenheder, S., 2021. Microbial community resilience across ecosystems and multiple disturbances. *Microbiol. Mol. Biol. Rev.* 85 (2), 10–1128. <https://doi.org/10.1128/MMBR.00026-20>.
- Price, G.W., Langille, M.G., Yurgel, S.N., 2021. Microbial co-occurrence network analysis of soils receiving short-and long-term applications of alkaline treated biosolids. *Sci. Total Environ.* 751, 141687. <https://doi.org/10.1016/j.scitotenv.2020.141687>.
- Quast, C., Pruesse, E., Yilmaz, P., Gerken, J., Schweer, T., Yarza, P., Peplies, J., Glöckner, F.O., 2012. The SILVA ribosomal RNA gene database project: improved data processing and web-based tools. *Nucleic Acids Res.* 41 (D1), D590–D596.
- Radl, V., Simoes-Araujo, J.L., Leite, J., Passos, S.R., Martins, L.M.V., Xavier, G.R., Rumjanek, N.G., Baldani, J.I., Zilli, J.E., 2014. Microvirga vignae sp. nov., a root nodule symbiotic bacterium isolated from cowpea grown in semi-arid Brazil. *Int. J. Syst. Evol. Microbiol.* 64 (Pt 3), 725–730.
- Reardon, C.L., Strauss, S.L., Mazzola, M., 2013. Changes in available nitrogen and nematode abundance in response to Brassica seed meal amendment of orchard soil. *Soil Biol. Biochem.* 57, 22–29. <https://doi.org/10.1016/j.soilbio.2012.07.015>.
- Röttgers, L., Faust, K., 2018. From hairballs to hypotheses—biological insights from microbial networks. *FEMS Microbiol. Rev.* 42 (6), 761–780. <https://doi.org/10.1093/femsre/fuy030>.
- Sah, S., Krishnani, S., Singh, R., 2021. Pseudomonas mediated nutritional and growth promotional activities for sustainable food security. *Curr. Res. Microb. Sci.* 2, 100084. <https://doi.org/10.1016/j.crmicr.2021.100084>.
- Shen, K., Li, L., Wei, S., Liu, J., Zhao, Y., 2024. A network meta-analysis on responses of forest soil carbon concentration to interventions. *Ecol. Process.* 13 (1), 41. <https://doi.org/10.1186/s13717-024-00414-1>.
- Stone, B.W., Dijkstra, P., Finley, B.K., Fitzpatrick, R., Foley, M.M., Hayer, M., Hofmockel, K.S., Koch, B.J., Li, J., Liu, X.J.A., Martinez, A., 2023. Life history strategies among soil bacteria—dichotomy for few, continuum for many. *ISME J.* 17 (4), 611–619.
- Storey, S., Ashaari, M.M., Clipson, N., Doyle, E., De Menezes, A.B., 2018. Opportunistic bacteria dominate the soil microbiome response to phenanthrene in a microcosm-based study. *Front. Microbiol.* 9, 2815. <https://doi.org/10.3389/fmicb.2018.02815>.
- Thompson, L.R., Sanders, J.G., McDonald, D., Amir, A., Ladau, J., Locey, K.J., Prill, R.J., Tripathi, A., Gibbons, S.M., Ackermann, G., Navas-Molina, J.A., 2017. A communal catalogue reveals Earth's multiscale microbial diversity. *Nature* 551 (7681), 457–463.
- Tian, L., Wang, X.W., Wu, A.K., Fan, Y., Friedman, J., Dahlin, A., Waldor, M.K., Weinstock, G.M., Weiss, S.T., Liu, Y.Y., 2020. Deciphering functional redundancy in the human microbiome. *Nat. Commun.* 11 (1), 6217. <https://doi.org/10.1038/s41467-020-19940-y>.
- Trivedi, P., Delgado-Baquerizo, M., Anderson, I.C., Singh, B.K., 2016. Response of soil properties and microbial communities to agriculture: implications for primary productivity and soil health indicators. *Front. Plant Sci.* 7, 990. <https://doi.org/10.3389/fpls.2016.00990>.
- Vitousek, P.M., Mooney, H.A., Lubchenco, J., Melillo, J.M., 1997. Human domination of Earth's ecosystems. *Science* 277 (5325), 494–499. <https://doi.org/10.1126/science.277.5325.494>.
- Vlassi, A., Nesler, A., Perazzoli, M., Lazazzara, V., Büschl, C., Parich, A., Puopolo, G., Schuhmacher, R., 2020. Volatile organic compounds from *Lysobacter capsici* AZ78 as potential candidates for biological control of soilborne plant pathogens. *Front. Microbiol.* 11, 1748. <https://doi.org/10.3389/fmicb.2020.01748>.
- Wang, X., Wang, Z., Zhang, Z., Yang, Y., Cornell, C.R., Liu, W., Zhang, Q., Liu, H., Zeng, J., Ren, C., Yang, G., 2023. Natural restoration exhibits better soil bacterial network complexity and stability than artificial restoration on the Loess Plateau, China. *J. Environ. Manag.* 346, 119052. <https://doi.org/10.1016/j.jenvman.2023.119052>.
- Weiss, S., Van Treuren, W., Lozupone, C., Faust, K., Friedman, J., Deng, Y., Xia, L.C., Xu, Z.Z., Ursell, L., Alm, E.J., Birmingham, A., 2016. Correlation detection strategies in microbial data sets vary widely in sensitivity and precision. *ISME J.* 10 (7), 1669–1681.
- Xiao, Z., Zhang, S., Yan, P., Huo, J., Aurangzeib, M., 2022. Microbial Community and Their Potential Functions after Natural Vegetation Restoration in Gullies of Farmland in Mollisols of Northeast China. *Land* 11 (12), 2231. <https://doi.org/10.3390/land11122231>.
- Yang, X., Jiang, N., Sun, D., 2024. Dry–wet cycles induce the decoupling of carbon and nitrogen mineralization at high temperatures in semi-arid grassland soil. *Soil Biol. Biochem.* 188, 109227. <https://doi.org/10.1016/j.soilbio.2023.109227>.
- Yasmeen, T., Aziz, A., Tariq, M., Arif, M.S., Shahzad, S.M., Riaz, M., Javed, A., Ali, S., Rizwan, M., 2021. Pseudomonas as plant growth-promoting bacteria and its role in alleviation of abiotic stress. *Plant Growth-Promoting Microbes for Sustainable Biotic and Abiotic Stress Management*, pp. 157–185. https://doi.org/10.1007/978-3-030-66587-6_7.
- Yu, Y., Shi, Y., Li, M., Wang, C., Zhang, L., Sun, Z., Lei, B., Miao, Y., Wang, W., Liu, B., Zheng, J., 2022. Land-use type strongly affects soil microbial community assembly process and inter-kingdom co-occurrence pattern in a floodplain ecosystem. *Appl. Soil Ecol.* 179, 104574. <https://doi.org/10.1016/j.apsoil.2022.104574>.
- Zhou, J., Deng, Y., Luo, F., He, Z., Yang, Y., 2011. Phylogenetic molecular ecological network of soil microbial communities in response to elevated CO₂. *e00122-11 mBio* 2 (4). <https://doi.org/10.1128/mBio.00122-11>.